Enrichment of halogenated organic compounds and their degrading microorganisms in the deepest ocean

Rulong Liu[1*], Hui Wei[1#], Zhiao Xu[1#], Yuheng Liu[1], Zhixuan Wang[1], Jiani He[1], Min Luo[1], Federico Baltar[1, 2], Yunping Xu[1], Qirui Liang[1], Liting Huang[1], Li Wang[1*], Jiasong Fang[1, 3, 4*]

[1] College of Oceanography and Ecological Science, Shanghai Ocean University, Shanghai, China

[2] Department of Functional and Evolutionary Ecology, University of Vienna, Vienna, Austria

[3] Laboratory for Marine Biology and Biotechnology, Qingdao National Laboratory for Marine Science and Technology, Qingdao, China

[4] Department of Natural Sciences, Hawaii Pacific University, Honolulu, HI, USA

***Correspondence:**

Rulong Liu, rlliu@shou.edu.cn

Li Wang, wang-l@shou.edu.cn

Jiasong Fang, jsfang@shou.edu.cn

[#], these authors contribute equally.

Abstract

The hadal trenches, the deepest regions of the ocean, serve as the final resting place for marine particles and as "tunnels" for material exchange between the ocean and Earth's interior. Despite their extreme conditions, the trenches contain high content of organic carbon (OC) and active microbial carbon turnover, are hotspots for deep-sea OC degradation and unique microbial processes. However, little is known about the OC components and microbial metabolisms driving the OC degradation in the trenches. This study reveals unexpectedly high concentrations of halogenated organic compounds (HOCs) in the Mariana Trench sediments, with about 1 halogen per 58 carbon atoms in the OC pool. Systematic analysis of deep-sequenced metagenomes and metagenome-assembled-genomes from the global ocean shows significantly higher abundance of the genes for biodegradation of HOCs (dehalogenation) in trench microbes, with microorganisms capable of dehalogenation belonging to 16 phyla and 52 orders, 75% of which identified as HOCs degraders for the first time. Microcosms simulating trench conditions showed rapid degradation of typical HOCs and transcription of genes related with HOCs metabolisms, demonstrating the active HOCs degradation by the trench microorganisms. The findings suggest the HOCs metabolism as an important process in the OC remineralization of deep-sea trenches, advancing understanding of deep-sea carbon cycling and microbial survival strategies.

Introduction

The deep ocean, covering 65% of the Earth's surface and housing 75% of the ocean's prokaryotic biomass, plays a crucial role in the remineralization and long-term storage of marine organic carbon [1]. However, our understanding of the metabolism of deep-sea microorganisms and the carbon turnover processes they drive remains limited, especially concerning carbon cycling in the ocean's deepest regions, known as hadal trenches. The hadal trenches, which are found at depths exceeding 6,000 meters, are among the most inaccessible and least understood marine environments on the planet [2, 3]. Located in subduction zones, the hadal trenches serve as both the endpoint for sinking organic matter from the upper ocean and as a "channel" for material exchange between the ocean and the Earth's deep interior [3]. Recent studies have shown that the hadal zone is rich in organic matter and exhibits unexpectedly active microbial organic carbon turnover, emerging as “hotspots” for organic carbon remineralization in the deep ocean [2, 4]. Furthermore, the extreme conditions of the hadal zone, such as high pressure and geographic isolation, have led to the development of unique microbial communities and special metabolic processes, forming a distinct "trench biosphere" [5, 6]. Understanding the processes and mechanisms by which hadal microbes drive the degradation of sedimentary organic carbon is essential for advancing knowledge of carbon cycling and life processes in deep-sea environments [2, 3].

While studies have demonstrated that hadal trench microorganisms exhibit potential for chemoautotrophic metabolism such as ammonia oxidation [7], metagenomic and genomic analyses suggest that microbial taxa present in the trench sediment predominantly adopt a heterotrophic lifestyle, possessing metabolic genes and

pathways for degradation of a wide range of organic matter, including simple sugars, peptides, fatty acids, proteins and other organic detritus [6, 8]. Particularly, most of the studies demonstrated the metabolic potential of hadal trench microbes to utilize multiple complex and recalcitrant organic compounds, such as hydrocarbons, polysaccharides and aromatic compounds [6, 8]. These findings are consistent with the higher humification of organic carbon in the bottom of hadal sediments [9], suggesting that the utilization of recalcitrant organic carbon might be a crucial metabolic strategy for hadal microbes [8, 10]. However, only a limited number of these metabolic processes, such as hydrocarbon degradation, have been experimentally validated combined evidences of biogeochemical detection of substrates and the assessment of microbial degradation activities [11, 12]. Due to the diverse and variable sources of organic matter[3], along with the unique biological, geological, and physicochemical factors regulating the dynamics of materials in hadal trenches [13, 14], the composition of organic matter in hadal sediments is highly complex. Consequently, our understanding of the components of organic carbon (OC) in hadal trenches and the microbial processes driving OC degradation in these sediments remains limited.

Halogenated organic compounds (HOCs) are widely recognized as environmentally hazardous substances, raising significant global concerns. As persistent organic pollutants, most anthropogenic HOCs exhibit high toxicity to various organisms and a strong tendency to bioaccumulate, causing considerable harm to the marine ecosystems [15]. In addition to human sources, large quantities of natural HOCs are also produced through various biological and abiotic processes [16, 17]. The ocean, being rich in halogen atoms, serves as the largest source of natural HOCs on Earth [18], with high level of HOCs detected in sinking particles [19]. Due to their recalcitrant nature, HOCs

are thought to be transported to the deep ocean via mechanisms such as biological pump and ultimately sequestered in deep-sea sediment [15, 19, 20]. However, little is known about the content of HOCs and their fate in the deep ocean.

Hadal trenches serve as major depositories of different types of pollutants [21, 22]. Recent studies have identified a variety of HOCs, such as organochlorine pesticides dichlorodiphenyltrichloroethane (DDT) and chlordane, industrial pollutants PCB and polybrominated diphenyl ethers (PBDE), in the macro-organisms and sediments of the Mariana Trench [22, 23, 24, 25]. In addition, our previous work revealed that genes encoding complete metabolic pathways for HOCs degradation are present in genomes of hadal Chloroflexi, one of the dominant taxa in in trench sediments [10, 26]. The finding suggests the possibility of microbial HOCs degradation in the hadal trench sediment. Nevertheless, the metabolic processes, degradation activities as well as the significance of the HOCs degradation in hadal trench carbon cycling is not explored. In this study, we applied an optimized combustion-IC based approach to determine the content and composition of total HOCs in sediments of the Mariana Trench. Surprisingly, the results revealed that the total HOCs represent a large proportion of OC pool in the trench sediments. Systematic metagenomic and genomic analysis further showed that genes encoding enzymes and pathways for HOCs degradation are enriched and prevalent in hadal trenches sediments, and are widely distributed across more than half of the microbial taxa. Microcosm experiments simulating trench conditions further demonstrated active degradation of HOCs by trench microbial communities. These findings provide novel insights into the significance of HOCs and their microbial degradation processes in carbon cycling of the hadal zone.

Results and Discussion

High content of HOCs in hadal trench sediments

A method based on combustion-ion chromoatography were developed and optimized to show high accuracy, precision and reproducibility in determining the content of adsorbable organic halogens (AOX) including fluorine, chlorine and bromine (AOF, AOCl, AOBr), and the corresponding insoluble organic halogens (IOF, IOCl, IOBr, IOX), as well as total organic halogen contents (TOBr, TOCl, TOF, TOX) in marine sediments [27]. In this study, the content and composition of HOCs were determined in 38 sediment samples of 4 sediment cores taken from 5842-10901 meters of the Mariana Trench, which resulted in a total number of 430 data points of different components of HOCs (Fig. 1; Fig. S1; Table S1). The results showed that HOCs presented in all of the trench sediments tested (Fig. 1B). The values of AOX, which indicates dissolved HOCs adsorbable by activated carbon, ranged from 4.90±0.70 to 383.14±64.17 mg/kg, while the insoluble HOCs (IOX) ranged from 71.82±0.50 to 459.96±21.90 mg/kg (Fig. 1B), were significantly higher than the content of AOX ($p < 0.01$, t-text). The dissolved fraction of HOCs were mainly dominated by organic chlorine compounds (AOCl), which were significantly more abundant than AOBr and AOF. In contrast, organic fluorine compounds (IOF) showed the highest abundance in the insoluble HOCs, followed by IOCl (Fig. 1B). Organic bromine compounds showed the lowest abundance in both the dissolved and insoluble HOCs (Fig. 1B). The concentration of total organic halogen (TOX) in sediments of the Mariana Trench ranged from 110.33 ± 2.71 to 594.15 ± 15.28 mg/kg, with an average value of 292.47 mg/kg (Fig. 1B). Although hydrocarbons and lipid biomarkers, e.g. alkanes, carboxylic acids, alcohols and GDGTs, have been reported to be potential components in OCs of hadal trench sediments, these compounds generally showed low abundance

(up to 15 mg/kg) [11, 12, 28]. HOCs determined in this study were at least one magnitude higher than the reported OC compounds, making HOCs the largest known component of organic matter in hadal trench sediments. The contents of total organic carbon were relatively stable in the tested samples, ranged from 0.48 – 0.69% (0.57 ± 0.06 %) (Fig. 1B). As a result, the calculated molar ratios of carbon to halogen atoms (C:X) were ranged from 17.8 to 121.8, with an average value of 49.2. This indicates an average of one halogen atom for every 49.2 organic carbon atoms, suggesting a high proportion of HOCs within the organic carbon pool in the tested trench sediments. Currently, understanding on components of deep-sea organic matter is scarce, and to the best of our knowledge, only one existing study reported the TOX values in the deep ocean and from only two stations [27]. The values of TOX in sediments of the MT were significantly higher than those reported in coastal and other deep-sea regions, despite the lower TOC content in the trench sediments (Fig. S2) [27]. Consequently, the proportion of HOCs were significantly higher in organic carbon of the trench sediments than those in the coastal or other deep-sea sediments (evidenced by the lower C:X ratio) (Fig. S2).

HOCs in marine environments might be natural or anthropogenic sourced [17, 18]. The hadal trenches have been reported to accumulate many types of manmade pollutants such as black carbon [29], mercury [30], and plastics [21]. It was therefore not surprising to have the anthropogenic HOCs in the trenches, and indeed, various types of anthropogenic HOCs, such as PCBs, PBDEs, and halogenated organic pesticides have been reported in animals of several trenches, including the MT [22, 23, 24, 31]. However, the reported anthropogenic HOCs generally showed low concentration in the trench sediment, with average values ranged from 0 to 2 μg/kg [22, 23, 24]. Our results showed

175 that the concentration of TOX were magnitudes higher than all of the reported
176 anthropogenic HOCs, suggesting that large amount of HOCs might be come from
177 other sources. Carbon isotopic compositions (δ13C) of TOC ranged between -20.0 to -
178 22.6 ‰, with an average value of -21.4 ‰ in the sediments analyzed (Fig. 1B), which
179 indicating that the organic matter in the sediments of the MT was mainly marine
180 sourced [32]. Such finding was consistent with conclusions driven by previous studies
181 carried out in the same region using the carbon isotopic or biomarker evidences [32, 33].
182 Marine sourced HOCs might therefore be an important contributor for the measured
183 high content of total HOCs in the hadal sediment of the MT. In fact, previous studies
184 have shown that HOCs can be formed biologically via synthesis of marine organisms
185 or abiotically via physical/chemical halogenation of natural organic matter in seawater
186 [17, 18, 19], and that the marine particles can be a natural sink for HOCs [19]. The TOX
187 values determined in the trench sediments here were comparable with those in deep-
188 sea particles (180-694 mg/kg) [19], supporting the potentials of contribution from
189 marine particles.
190
191 **Enrichment of dehalogenase in sediments of the Mariana Trench**
192 HOCs are typically considered to be resistant to microbial degradation [16]. The
193 potential for microorganisms residing in hadal trench sediments to metabolize and
194 degrade HOCs was investigated through a comprehensive metagenomic analysis
195 focusing on the occurrence, relative abundance, and distribution of dehalogenase,
196 which is the key enzyme for the biodegradation of HOCs [34, 35, 36]. A total of 54
197 metagenomes from global ocean sediments were examined, comprising 27 deeply
198 sequenced metagenomes from sediment cores collected from depths of 5,437 to
199 10,954 meters in the Mariana Trench, alongside 27 metagenomes from other deep-sea

200 and shallow coastal sediments (Fig. 1A, Table S2). Following sequence preprocessing
201 and functional annotation against the KEGG database, various types of dehalogenase
202 genes were identified and validated through BLASTP search against the UniProt
203 protein database. The relative abundance of these confirmed dehalogenase genes was
204 quantified and expressed as genes per million (GPM). The results indicated the
205 presence of dehalogenases in all metagenomes derived from Mariana Trench
206 sediments (Fig. 2A). Specifically, four distinct types of dehalogenases were identified:
207 haloalkane dehalogenase, S-2-haloacid dehalogenase, haloacetate dehalogenase, and
208 reductive dehalogenase (Fig. 2A). These enzymes facilitate the biodegradation of
209 various HOCs through either hydrolytic or reductive mechanisms [18], suggesting a
210 significant metabolic versatility regarding HOCs within trench sediments. Notably,
211 the relative abundance of haloalkane dehalogenase and S-2-haloacid dehalogenase
212 was significantly higher in Mariana Trench sediments compared to other deep-sea and
213 shallow sediments ($p < 0.001$, t-test) (Fig. 2A), indicating an enrichment of
214 dehalogenation metabolism within the microbiome of the Mariana Trench. These
215 results align with the high levels of HOCs found in the sediment of the trench (Fig.
216 1B), implying that trench microorganisms may utilize HOCs as substrates for living.
217 Furthermore, phylogenetic analysis of 2,300 haloalkane dehalogenase sequences from
218 the Mariana Trench metagenomes, in conjunction with all manually annotated and
219 non-redundant haloalkane dehalogenase sequences available in the UniProt-Swiss
220 database, revealed that the microbial communities in the Mariana Trench encompass
221 all three types of haloalkane dehalogenases (HDL-I, II, and III) (Fig. 2B). This
222 suggests functional complementation among these enzymes, as different types of the
223 enzyme exhibit varying substrate specificities [37]. Interestingly, the sequences derived
224 from the trench metagenomes formed unique clusters that were distinct from known

225 haloalkane dehalogenases (Fig. 2B), indicating the presence of novel phylotypes that
226 may possess unique structural and functional characteristics, which were potentially
227 resulting from long-term adaptation to the extreme environmental conditions of the
228 hadal trench, such as low temperatures and high pressures [2, 3].
229

230 **Prevalence of dehalogenation metabolism among hadal trench microorganisms**

231 In this study, a total of 2544 metagenome-assembled-genomes (MAGs) were
232 reconstructed from the 27 metagenomes derived from the Mariana Trench sediments.
233 After dereplication at 95% average nucleotide identity (ANI), 285 representative
234 genomes were obtained. Functional annotation and homology confirmation revealed
235 that over half of the trench microbial taxa, specifically 50.2% (143 MAGs), harbored
236 genes encoding dehalogenases (Fig. 2A; Table S3). These MAGs showed
237 contamination < 4.99%, the genome size ranged from 0.58 to 5.31 Mbp, the GC
238 content ranged from 59.4 to 65.4%, and 79 of them had a genome completeness
239 greater than 80% (Fig. 2A; Table S3). Among the 143 MAGs, 78 MAGs contained
240 genes for S-2-haloacid dehalogenase, 11 for haloacetate dehalogenase, 79 for
241 haloalkane dehalogenase, and 23 for reductive dehalogenase. While the majority of
242 the MAGs harbored a single type of dehalogenase, 40 MAGs contained genes for
243 multiple dehalogenase types, with one MAG from the Chloroflexota phylum
244 (MT_10840m_10-14cm.31) possessing genes for all four dehalogenases (Fig. 2A).
245 Phylogenomic analysis and taxonomic classification against the GTDB database
246 revealed that the 143 MAGs with dehalogenation potentials were distributed across 16
247 bacterial phyla and 20 classes, including 60 novel species and 15 novel genera (Fig.
248 2A; Table S3). By comparing against the mibPOPdb database, which is a manually
249 curated integrative resource for microbial bioremediation of persistent organic

250 pollutants (POP) [38, 39], 11 of the 16 phyla were reported to have the capability of
251 dehalogenation for the first time (Fig. 2A), thereby greatly enhancing the current
252 understanding of the diversity of dehalogenation microorganisms. The MAGs
253 encoding dehalogenases were found to be widely distributed across all analyzed MT
254 sediment samples, with the total relative abundance of dehalogenation
255 microorganisms constituting between 8% and 21% of the metagenome reads (Fig.
256 2B). Majority of the MAGs (96 MAGs) showed high occurrence frequency, being
257 present in over 80 % of the MT sediment samples (Fig. 2B, Table S4). These findings
258 suggest that the dehalogenation microorganisms were both prevalent and dominant in
259 the microbial communities of the trench sediments.
260
261 Functional annotation utilizing the KEGG, COG, and PROKKA databases revealed
262 that the dehalogenation population, represented by the 143 dehalogenation MAGs,
263 contained gene sets that encode pathways for the degradation of various HOC
264 compounds with distinct molecular structures. Specifically, the population was
265 associated with the degradation of 18 compounds categorized into groups such as
266 chlorocyclohexane and chlorobenzene, chloroalkane and chloroalkene,
267 fluorobenzoate, as well as polychlorobiphenyl (PCB) (Fig. 3, Fig. S3, Table S5).
268 These represent nearly all documented degradation pathways for HOCs in the KEGG
269 database, suggesting the wide range of substrate spectra for the dehalogenation
270 population identified in hadal trench environments. Majority of the HOCs compounds
271 (15 of 18), e.g. γ- hexachlorocyclohexane, 2,6-dichloropenol, 2,4-
272 dichlorophenoxyaceate, 2,4-dichloroaniline, cis-dichloropropene, trans-
273 dichloropropene, 1,2-dichloroethane, dichloromethane, 2-fluorobenzoate, 3-
274 fluorobenzoate, 4-chlorobenzoate, and 4-chlorobiphenyl, could be completely

275 degraded via entering the TCA cycle (Fig. 3, Table S5). Furthermore, coding genes for
276 each of the functional enzymes involved in these degradation pathways was identified
277 across various genomes from multiple phyla (Fig. 3, Table S5), indicating a functional
278 redundancy that facilitates the efficient degradation of substrates [40]. The exact
279 molecular composition of HOCs present in trench sediment remains undetermined.
280 Nevertheless, as previously discussed, they are hypothesized to comprise a mixture of
281 both anthropogenic and natural HOCs. The anthropogenic HOCs are characterized by
282 low structural diversity [16], with majority of their degradation pathways being
283 annotated in our analysis (Fig. 3, Table S5). In contrast, natural HOCs exhibit a
284 considerably higher diversity in their molecular structures [16, 17]. However, as the
285 primary source of organic matter in deep-sea and hadal trenches, phytoplankton and
286 sinking particles have been identified as containing HOCs that were predominant by
287 aliphatic forms [19]. Considering the diverse degradation pathways identified in the
288 MAGs, the dehalogenation population possess the potential to efficiently utilize HOC
289 substrates present in hadal trenches.
290
291 In addition to direct degradation of HOCs, the dehalogenation population showed
292 potentials to contribute to other ecological functions. Firstly, the degradation
293 pathways of HOCs annotated involved were generally long, with many steps and
294 produce series of intermediates (Fig. 3). These intermediate compounds, with lowered
295 recalcitrancy compared to their original compounds, can also be substrates for other
296 heterotrophic taxa, supporting the potential role of the dehalogenation
297 microorganisms as mediators of microbial interactions within hadal trenches [16, 41].
298 Furthermore, the dehalogenation microbial populations also showed the capability to
299 drive the biogeochemical cycling of multiple key elements other than halogen and

carbon. Particularly, the sulfur oxidation seemed to be common in the dehalogenation population, with 49-87% of the MAGs harbored gene sets for different steps of sulfur oxidation (Fig. 3, Fig. S3, Table S5). Moreover, 43% and 45% of the MAGs also showed potentials of iron reduction and iron oxidation, respectively (Fig. 3, Fig. S3, Table S5). Overall, the findings demonstrate a significant role of dehalogenation microorganisms in the functions and structures of hadal trench ecosystems.

Active HOCs degradation driven by hadal trench microorganisms

The degradation activity of HOCs by hadal trench microorganisms was demonstrated by inoculating typical HOCs compounds—PCB and γ-HCH—into sediments from the Mariana Trench (MBR06, 6477 m depth) and incubating them for 270 days under high pressure (60 MPa) and low temperature (4 °C) to simulate *in-situ* conditions. Time-series sampling and monitoring revealed a rapid decrease of substrate abundance in all treatments containing trench microorganisms (non-sterile systems), whereas no significant changes occurred in the control systems (sterile sediments) (Fig. 4A). For both substrates, the most substantial decrease took place within the first 30 days, leaving less than 40% of the original material. PCB levels continued to decline throughout the 270-day period, whereas γ-HCH remained relatively stable after day 30. Reads recruited to metagenomes and metatranscriptomes indicated that the dehalogenation population, i.e., the 143 MAGs with dehalogenation potential, were present and actively expressed in the microcosms (Fig. 4B). Dominant dehalogenation MAGs included those from the orders UBA1845 (p_Planctomycetota), Hydrogenedentiales (p_Hydrogenedentota), SAR324 (p_SAR 324), Longimicrobiales (p_Gemmatimonadota), UBA5794 (p_Actinomycetota), UBA9160 (p_Myxococcota), Woeseiales, Pseudomonadales, Kiloniellales

(p_Proteobacteria), and SM23-28-2, UBA1151, SAR202, UBA3496, DSTF01 (p_Chloroflexota) (Fig. 4B). Among these, MAGs from the order Pseudomonadales were the most abundant in the microcosms (Fig. 4B). The majority of functional genes associated with HOC degradation pathways were found in high relative abundance in the metagenomes of the microcosms (Fig. 4C, Table S6), with over half of these genes being actively expressed in the transcriptome (Fig. 4D, Table S6). Notably, genes such as *dhaA*, *EC:1.1.1.1*, *clcD*, *catB*, *EC1.14.13.-*, and *ALDH*, which encode haloalkane dehalogenase, alcohol dehydrogenase, carboxymethylenebutenolidase, muconate cycloisomerase, 2-octaprenylphenol hydroxylase, and aldehyde dehydrogenase, respectively, exhibited high transcriptional abundance (Fig. 4D). Overall, the results from the chemical and microbial analyses in the microcosm experiments indicated rapid degradation of typical HOCs, alongside active expression of microorganisms and functional genes related with dehalogenation metabolism. This suggests that hadal trench microorganisms actively metabolize HOC under the high pressure and low temperature conditions. However, this cultivation experiment was limited to two specific human-made halogenated organic compounds. Future research is necessary to explore the metabolic activity of deep-sea microorganisms on other types of HOCs, particularly natural ones. Additionally, since this experiment utilized enriched sediment microorganisms in a laboratory setting, the degradation rates observed may differ from those in natural environments. Future in-situ cultivation studies are needed for a more accurate evaluation of the degradation rates and flux of HOCs.

Implications for deep-sea biogeochemical cycling and environmental bioremediation

The deep-sea environments constitute a significant portion of the Earth's microbial biomass and production, thereby playing a crucial role in regulation of global carbon cycling and climate change[1]. However, there remains a limited understanding of the metabolic processes of deep-sea microorganisms and the carbon turnover mechanisms they facilitate. On the other hand, over the past few decades, dehalogenation processes and the microorganisms involved have attracted a wide range of research interests, primarily due to their potential applications in the bioremediation of dioxin pollutants [42]. Nevertheless, their ecological roles in carbon cycling of the natural environments have largely been overlooked [16, 41]. This study presents novel evidence showing a surprisingly high concentration of HOCs within the TOC pool of deep-sea trenches. It also highlights the enrichment and prevalence of HOCs metabolic potentials across a diverse array of microbial taxa, as well as the active degradation of typical HOCs by microorganisms in the Mariana Trench under simulated *in-situ* conditions. These results indicate that HOCs may serve as important substrates for microorganisms inhabiting trench environments, and that the metabolism of HOCs may represent a common strategy for the survival of microorganisms in harsh conditions of the hadal trenches, such as the presence of recalcitrant organic matter. The findings not only enhance the current understanding of microbial processes and survival strategies in extreme marine environments, but also underscore the significance of HOCs degradation in the microbial carbon turnover in the Mariana Trench. Given that trenches are "hotspots" for microbial carbon turnover and early diagenesis in the deep ocean [4], the observed active degradation process of HOCs in the MT sediments is believed to have great contribution to the deep-sea organic carbon remineralization. Furthermore, our results also showed that dehalogenases present in all of the microbial metagenomes from various habitats across the global

ocean (Fig. 2), with potential dehalogenation microorganisms, such as Chloroflexi, being widespread and dominant in the sediments of the hadal trenches and other deep ocean habitats [43, 44]. Dehalogenation activities have even been recorded in deep subseafloor sediments down to 358 m below the seafloor [45, 46]. Although research on this topic remains limited, existing evidence suggests that HOC metabolism is likely widespread in deep-sea environments. This implies that the microbial degradation of HOCs may play an important yet overlooked role in the global deep-sea carbon cycle, warranting further investigation in future studies.

Conversely, HOCs have been regarded as hazardous pollutants pose substantial environmental risks, and they are believed to ultimately become sequestered in deep-sea sediments due to their persistent nature [15, 20]. The findings of this study demonstrate that HOCs can serve as substrates for a diverse array of microbial taxa in deep-sea environments, where they can be effectively degraded. This provides valuable new insights into the fate and environmental implications of HOCs within deep-sea ecosystems. Additionally, the high diversity of dehalogenation microorganisms along with the unique phylogenetic traits of dehalogenase identified in hadal trenches, represent promising resources for bioremediation efforts.

Material and Methods

Sampling sites and sample processing

Sediment samples from MBR02 (11.327°N,142.188°E, water depth 10901 m), MBR04 (10.761°N,142.274°E, water depth 5842 m), MBR05 (10.979°N, 141.950°E, water depth 6957), and MBR06 (10.813°N,141.180°E, water depth 6477 m) of the Mariana Trench were taken during the R/V *Tansuoyihao* TS15 cruise on December

2019 (Fig. 1). Samples were taken by a box corer attached to a Hadal Lander. The procedures of the sample processing were the same as in [10, 26]: after recovering onboard, the sediment samples were immediately subsampled using sterile polypropylene corers, and most of the cores were stored under -80 °C until analysis. The pore water was collected at 1–2 cm intervals using Rhizon samplers. Aliquots for DOM analysis were stored in a pre-combusted (525 °C for 4 h) brown glass bottle, sealed with an acid-cleaned Teflon-lined cap, and frozen at −20 °C.

Measurement of halogenated organic matter and geochemical parameters

The method for sample pretreatment and HOCs measurement followed our previous study Wei et al.,[27]. Briefly, sediment cores for HOCs measurement were thawed and divided at 2 cm interval along the vertical depth profile. The most outer layer of each depth fraction was removed to avoid halogen contamination, and the remaining sample was freeze-dried and ground. Twenty milligram sediment was then weighted out from each sample and mixed with 50 mL sodium nitrate washing solution, shaking for 2 h at 140 rpm and then stay overnight to remove inorganic halogens [27]. The sediment slurry was then filtered through a polycarbonate (PC) membrane to collect insoluble fraction of the sediment. Eighty milligram of activated carbon was added to the filtrate and shake for 2 h at 140 rpm. The activated carbon with dissolved organic matter adsorbed was collected on a PC membrane by filtration. The two PC membranes were then subject to combustion for measurement of content of insoluble and absorbable HOCs, respectively. The protocols for combustion and detection of different halogen ions by IC were the same as Wei et al., [27]. All labware utilized were carefully selected and pretreated according to Wei et al. (2024) to secure that they were free of halogen contamination. Three replicates were taken for each sample.

Triplicate sample processing blanks and analytical blanks were involved in each batch of experiment to indicate the presence and level of the background contamination. All measured values were calibrated by subducting the background values in blank controls from the same batch of experiment.

Content of TOC (wt.%) was determined with a TOC analyzer (Multi N/C 3100 Analytik Jena) according to the procedure of Xu et al. [47]. Carbon isotopic composition of TOC was determined according to Luo et al., [32], using high temperature combustion on a Vario Pyro Cube Elemental Analyzer connected to an Isoprime 100 Continuous Flow Isotope Ratio Mass Spectrometer. Stab le isotope results were reported using the per mil notation (δ, ‰) relative to the V-PDB standard. Pore-water DOC concentrations were determined by a high-temperature catalytic combustion method using a Shimadzu TOC-L total carbon analyzer with a precision of ±3% [9]. Inorganic nutrients (NO_3^-, NO_2^-, NH_4^+, and PO_4^{3-}) were determined using a QuAAtro autoanalyzer (Seal Analytical, United Kingdom) [48].

Metagenomic sequencing and public data collection

Sediment cores were thawed on ice and were depth fractioned at 5 cm intervals (2019 cruise). Total genomic DNA was extracted from 10-20 g of sediments from each depth fraction using the PowerMax® Soil Kit (MoBio Laboratories, USA), and then purified by DNeasy® PowerClean Pro Cleanup Kit (Qiagen, Germany). DNA fragment libraries were prepared by shearing genomic DNA from each sample and were then subjected to metagenomic sequencing on the illumine MiSeq platform in Majorbio Bio-Pharm Technology Co. Ltd (Shanghai, China). In total, 8 metagenomes

were successfully sequenced and generated 335.4 Gb of raw reads. The data size for individual metagenomes ranged from 27.2 - 50.1 Gb, with an average value of 41.9 Gb. The metagenomes were combined with 46 additional deep-sequenced metagenomes from NCBI database (including 19 metagenomes from sediments of the Mariana Trench and 27 from other habitats of the global ocean) (Table S1), and were co-analyzed for distribution of dehalogenase and related microorganisms.

Assembly, functional annotation, and dehalogenase genes identification

Metagenomic reads from each sample were quality filtered using Trimmomatic v. 0.38 [49] with parameters specified as "LEADING:30 TRAILING:30 CROP:90 HEADCROP:10 SLIDINGWINDOW:4:25 MINLEN:50," and were separately assembled with metaSPAdes v. 3.15.5 (-m 700) [50]. Gene predictions were performed against the assembled contigs using Prodigal v. 2.6.3 (-p meta) [51], and genes were then dereplicated to construct the non-redundant gene database using CD-HIT v. 4.8.1 with default parameters [52]. Functional annotation was performed using BlastKOALA against the KEGG database with default parameters [53]. The gene sequences annotated as any types of dehalogenases were extracted and confirmed using BLASTp search against UniProt protein database [54].Only the sequences showed ≥ 60% identity, ≥ 90% coverage and E values < 10^{-5} with existing dehalogenase sequences in the UniProt database were selected for downstream analysis.

Relative abundance determination and phylogenetic analysis of dehalogenase

Clean reads from each metagenome were mapped back to confirmed dehalogenase genes sequences using BWA v. 0.7.17 [55]. BWA output was then converted to a sorted and indexed bam file using SAMtools v. 1.9 [56].The number of mapped reads and

length of each gene sequence from the bam file was utilized for calculation of the length normalized gene abundance, which was expressed as GPM (genes per million). The relative abundance of each type of dehalogenase was calculated by summing the GPM values of the confirmed gene sequences.

Phylogenetic analysis was conducted to reveal the differences between the hadal trench dehalogenase and the existing counterparts. A total of 2300 BLASTP confirmed haloalkane dehalogenase gens sequences were extracted from the 28 Mariana Trench metagenomes, translated in to protein sequences, and co-analyzed with 37 previously characterized haloalkane dehalogenase sequences from the Uniport database. The sequences were aligned with MAFFT v. 7.467 [57] and trimmed with trimAl software [58], with default parameters. A maximum-likelihood phylogenetic tree was constructed with IQ-Tree [59]with 100 bootstrap replicates.

Genome binning and dereplication

The quality-filtered reads were mapped back to the assembled contigs using Bowtie2 (v. 2.3.4.1) [60], and coverage was determined according to the mapping results with the jgi_summa- rize_bam_contig_depths script [60]. Metagenome binning was conducted for assemblies longer than 2500 bp using MetaBAT v. 2.12.1 [61] with default parameters. Quality of the MAGs was assessed by CheckM v. 1.1.2 using the line-age_wf workflow [62], and only MAGs with completeness > 50% and contamination < 5% were kept for further analysis. Redundant bins were subsequently dereplicated using dRep v. 2.3.2 [63] at 95% average nucleotide identity (ANI) (all other parameters were set to the default), and MAG with the highest quality was selected from each cluster for downstream analysis. The genome size was estimated by dividing the size

500 of the MAG by its estimated completeness.

501

502 **Taxonomic assignment, identification of dehalogenation taxa and calculation of**

503 **their relative abundance**

504 Taxonomic classification of the MAGs was determined using GTDB-Tk, which is

505 based on the phylogenetically calibrated Genome Taxonomy Database (GTDB) [64].

506 Coding sequences in the MAGs were predicted using Prodigal v. 2.6.3 with default

507 setting [51]. Functional annotation was performed by using BlastKOALA against the

508 KEGG database with default parameters [53]. The annotation results were manually

509 examined to screen for the MAGs with dehalogenase annotated. The sequences of

510 dehalogenase genes were then extracted from each candidate MAG and confirmed

511 using BLASTp search against UniProt protein database. Only the MAGs containing

512 gene sequences showing ≥60% identity and ≥ 90% coverage with existing

513 dehalogenase in the UniProt database were selected as the potential dehalogenation

514 microorganisms.

515

516 Phylogenomic tree was constructed for the confirmed dehalogenation MAGs, using

517 the 43 universal single-copy genes (SCGs) used by CheckM [62]. Protein sequences of

518 the SCGs were identified using HMMER v. 3.1b2 [65] with default parameters,

519 individually aligned with MAFFT v. 7.467 [57] and then concatenated. Phylogenomic

520 tree was constructed based on the alignment using FastTree2 v. 2.1.11 [66], with a JTT

521 model, a gamma approximation and 100 bootstrap replicates. Archaeal genome

522 (GCF_004799605.1) was utilized as the root. The phylogenomic tree was visualized

523 with iTOL [67].

524

525 Relative abundances of the dehalogenation MAGs were calculated by mapping the
526 trimmed reads to the manually curated and refined MAGs with CoverM (v.0.6.1;
527 https://github.com/wwood/CoverM) in genome mode including the dereplication flag
528 using the default aligner Minimap2 (v.2.21; https://docs.csc.fi/apps/minimap2/) in
529 short-read mode, discarding unmapped reads. The final relative abundance of each
530 MAG is the percentage of the MAG in the mapped fraction of each sample.
531

532 **Reconstruction of metabolic network for dehalogenation microorganisms**

533 Systematic metabolic capabilities of the dehalogenation microbial taxa were explored
534 by systematic annotation of MAGs containing dehalogenase genes. Coding sequences
535 in the MAGs were annotated against the KEGG [53], Cluster of Orthologous Groups
536 (COG) [68], as well as PROKKA databases [69], following the steps in Liu et al. [10]. The
537 pathways related with energy metabolism and biogeochemical cycling were also
538 annotated with METABOLIC [70]. Metabolic network was reconstructed for each of the
539 MAGs by summarizing the annotated pathways.
540

541 Coding sequences in the MAGs were annotated against the KEGG[53], Cluster of
542 Orthologous Groups (COG)[68], as well as PROKKA databases[69], following the steps in
543 Liu et al.[10]. The pathways related with energy metabolism and biogeochemical
544 cycling were further annotated with METABOLIC[70]. Metabolic network was
545 reconstructed for each of the MAGs by summarizing the annotated pathways.
546

547 **High-pressure microcosms**

548 ***Microcosm set up and sampling***

549 Sediments were taken from site MBR06 (water depth 6477 m) of the Mariana Trench

using a box corer during RV Tansuoyihao TS15 cruise on December 2019. After removing the outer layers, around 2.0 kg sediment were taken by pre-combusted (450 °C, 4 h) stainless steel scoops. Sediment samples were transferred into sterile incubation bags (polypropylene) and stored under 4 °C for 20 months, which leads to the enrichment of dehalogenation microbial taxa (relative abundance of dehalogenation microbial taxa increased from < 20% to 53% of total mapped metagenomic reads).

After thorough mixing with a pre-combusted stainless steel scoop, the sediments were divided into polypropylene incubation bags and mixed with 0.2 μm filtered seawater taken from 6000m depth of the Mariana Trench. Each of the 50 ml incubation bag contained 15 g sediment and 30 ml filtration sterilized seawater, and then either 1.5 mg of 4-Chlorobiphenyl (4-PCB) or 3 mg of γ-Hexachlorocyclohexane (γ-HCH) was amended as the representatives of anthropogenic HOCs with low or high numbers of halogen atoms, respectively. No-substrate controls and no-microorganism controls were set up simultaneously with the experimental groups. No-substrate controls are incubation bags contained only sediment and sterilized seawater, and without halogenated organic matter substrates. No microorganism controls are incubation bags containing autoclaving sterilized sediments and filtration sterilized seawater, and either type of halogenated organic substrates with the same ratios as the experiment groups. All of the incubation bags for experimental groups and the controls were put into high pressure incubation vessels, and were incubated under 60 MPa and 4 °C to simulate the *in-situ* pressure and temperature. Triplicate incubation bags were taken for each treatment at day 0, day 30, day 60, day 90, and day 270 to monitoring the changes of organic substrates and microbial metabolisms.

575

576 ***4-PCB and γ-HCH measurement***

577 Around 15 mL of sediment slurry from each incubation bags were freeze dried and
578 ground. After mixing with 100 μL surrogate standard solution (2,4,5,6-Tetrachlorom-
579 xylene, 500 mg/L), the sample was transferred into Accelerated Solvent Extraction
580 (ASE) cells for extraction with (1:1, v/v) (72 °C, 20 h for 4-PCB, and 65 °C, 22h for
581 HCH). The yielded extract from each cell was then evaporated to a final volume of 1
582 mL and then cleaned up in CNWBOND Florisil PR SPE cartridge (60-100 mesh, 1
583 g/6 mL). First, 1 g of Na_2SO_4 was added to the cartridge and 10 mL of n-hexane was
584 added to pre-condition the column. Then the extract was transferred into the column
585 and eluted by 10 mL of acetone:n-hexane (1:1). The collected effluent was
586 concentrated to 5 mL. Before instrumental analysis, 100 μL of the effluent was
587 transferred into amber GC vials, and 50 μL of injection standard (50 mg /L, 1-Bromo-
588 2-nitrobenzene for 4-PCB analysis, Pentachloronitrobenzene for HCH analysis) was
589 added to calculate recoveries.

590

591 The 4-PCB and HCH were analyzed by using gas chromatograph (Agilent 7890B;
592 DB-5 column, 15m× 0.32mm×0.25 μm) equipped with 63Ni-ECD detector (for
593 analysis of HCH) and MSD detector (for analysis of PCB). Samples (1 μL) were
594 injected in the splitless injection mode with high purity nitrogen as carrier gas (1
595 mL/min for 4-PCB analysis, and 2 mL/min for HCH analysis). For analysis of 4PCB,
596 the temperature of the column was set at 40°C for 2 min, then raised to 280°C
597 (20°C·min^{-1}), and finally retained at 280°C for 5 min. The injection port and detector
598 temperatures were kept at 270°C and 280°C, respectively. For analysis of HCH, the
599 temperature of the column was set at 100°C for 2 min, raised to 220°C (15°C·min^{-1})

600 and retained for 5 min, then raised to 260 °C (15°C·min^{-1}) and retained for 20 min.
601 The injection port and detector temperatures were kept at 220°C and 300°C,
602 respectively.
603
604 The quality control steps included sample processing blanks, limit of detection,
605 recovery tests, replicates, and standard curves. Sample processing blanks were
606 involved for each batch of experiment to indicate possible contamination. All blanks
607 were below the limits of detection (LOD). The LODs were set to be triple the standard
608 deviation of the blanks, which were averagely 0.1 μg/g for PCB and 0.01μg/g for
609 HCH. Spiked recovery tests of the standards showed acceptable recoveries ranging
610 from 81.80% to 85.40% for 4-PCB, with the relative standard deviation (RSD) less
611 than ±2.57%, and from 91.59% to 94.63 % for HCH, with the RSD less than ±
612 4.74% . The standard curves had high degree of linearity ($R^2 > 0.999$) for all the
613 compounds.
614
615 ***Metagenomic and metatranscriptomic analysis***
616 Total DNA and RNA were coextracted from each of the microcosm samples using
617 PowerSoil Total RNA Isolation Kit and DNA Elution Accessory Kit (MoBio Lab,
618 United States). The concentration and quality of DNA and RNA were determined
619 using both Qubit 4.0 (Thermo Fisher Scientific, Waltham, USA) and Nanodrop One
620 (Thermo Fisher Scientific, Waltham, USA). Quality of RNAs were also determined
621 through the Agilent 4200 system (Agilent Technologies, Waldbronn,
622 Germany). All of the DNA samples were directly subject to library preparation using
623 the ALFA-SEQ DNA library Prep Kit (Findrop Biosafety Tech., China). The RNA
624 samples went through whole transcriptome amplification using RNA REPLI-g Cell

625 WGA & WTA Kit (Qiagen, Germany), and subject to library construction using
626 ALFA-SEQ RNA library Prep Kit II (Findrop Biosafety Tech., China). The DNA
627 libraries and RNA libraries were then subject to metagenome and metatranscriptome
628 sequencing, respectively, in Magigene Biotechnology Co. Ltd (Guangzhou, China)
629 using Illumina novaseq6000 (PE150 sequencing).
630
631 The sequencing was successful for all of the metagenomes. Metagenomic reads from
632 each sample were quality filtered, assembled, and genes were predicted and
633 dereplicated following the same procedure as mentioned earlier. Functional annotation
634 was performed against the KEGG, COG and PROKKA databases. The gene
635 sequences involved in any of the HOCs degradation pathways were extracted and
636 confirmed via BLASTp. Clean reads from each metagenome were mapped back to
637 predicted genes using BWA v. 0.7.17 and the gene length normalized relative
638 abundance of each gene were expressed as GPM. The relative abundances of the
639 dehalogenation genomes were estimated by mapping the metagenomic reads to
640 sequences of the corresponding MAGs and expressed as GPM.
641
642 Duplicated metatranscriptomes were successfully sequenced for both PCB and HCH
643 microcosm samples taken from 90th day. Metatranscriptomic raw reads were quality
644 filtered using Trimmomatic v. 0.38 [49], and non-coding RNAs were removed using
645 sortmerna v. 4.2.0 [71]. Clean reads of each metatranscriptome were then mapped to the
646 predicted protein coding genes of the metagenome from the same sample. The
647 transcription level of each gene was expressed as transcripts per million (TPM).
648 Similarly, the transcription level of the dehalogenation genomes was estimated by

mapping the metatranscriptome clean reads to sequences of the corresponding MAGs and expressed as TPM.

Acknowledgements

This work was supported by the National Natural Science Foundation of China (grant numbers 42276149, 92251303) and the Shanghai Frontiers Research Fund of the Hadal Biosphere. We also acknowledge organizers, technological teams and crews in the cruises of M.V. Zhangjian and R.V. Tansuoyihao.

References:

1. Herndl, G. J., Bayer, B., Baltar, F., Reinthaler, T. Prokaryotic life in the deep ocean's water column. Annu. Rev. Mar. Sci. **15**, 461–83 (2023).

2. Du M, et al. Geology, environment, and life in the deepest part of the world's oceans. Innovation (New York, NY) 2, 100109 (2021).

3. Jamieson A. The Hadal Zone: Life in the Deepest Oceans (2015).

4. Glud RN, et al. Hadal trenches are dynamic hotspots for early diagenesis in the deep sea. Communications Earth & Environment 2, 21 (2021).

5. Nunoura T, et al. Hadal biosphere: Insight into the microbial ecosystem in the deepest ocean on Earth. Proceedings of the National Academy of Sciences of the United States of America 112, E1230-E1236 (2015).

6. Zhou YL, Mara P, Cui GJ, Edgcomb VP, Wang Y. Microbiomes in the Challenger Deep slope and bottom-axis sediments. Nature Communications 13, 1515 (2022).

7. Thamdrup B, et al. Anammox bacteria drive fixed nitrogen loss in hadal trench sediments. Proceedings of the National Academy of Sciences of the United States of America 118, 46 (2021).

8. Chen P, et al. Revealing the full biosphere structure and versatile metabolic functions in the deepest ocean sediment of the Challenger Deep. Genome Biology 22, 207 (2021).

9. Hu TC, et al. Probing sedimentary DOM in the deepest sector of Earth's surface. Marine Chemistry 237,104033 (2021).

10. Liu RL, et al. Novel Chloroflexi genomes from the deepest ocean reveal metabolic strategies for the adaptation to deep-sea habitats. Microbiome 10, 1-17 (2022).

11. Guan H, et al. Composition and origin of lipid biomarkers in the surface sediments from the southern Challenger Deep, Mariana Trench. Geoscience Frontiers 10, 351-360 (2019).

12. Liu JW, et al. Proliferation of hydrocarbon-degrading microbes at the bottom of the Mariana Trench. Microbiome 7, 47 (2019).

13. Chu MF, et al. Earthquake-enhanced dissolved carbon cycles in ultra-deep ocean sediments. Nature Communications 14, 5427 (2023).

14. Jiang HC, et al. Three-layer circulation in the world deepest hadal trench. Nature Communications 15, 8949 (2024).

15. Sanganyado E, Chingono KE, Gwenzi W, Chaukura N, Liu WH. Organic pollutants in deep sea: Occurrence, fate, and ecological implications. Water Research 205, 117658 (2021).

16. Atashgahi S, Häggblom MM, Smidt H. Organohalide respiration in pristine environments: implications for the natural halogen cycle. Environmental Microbiology 20, 934-948 (2018).

17. Gribble GW. Naturally Occurring Organohalogen Compounds-A Comprehensive Review. Progress in the chemistry of organic natural products 121, 1-546 (2023).

18. Liu YH, Wang L, Liu RL, Fang JS. Biogeochemical cycling of halogenated organic compounds in the ocean: Current progress and future directions. Deep-Sea Research Part I-Oceanographic Research Papers 205, 104237 (2024).

19. Leri AC, et al. A marine sink for chlorine in natural organic matter. Nature Geoscience 8, 620-624 (2015).

20. Wagner CC, et al. A Global 3-D Ocean Model for PCBs: Benchmark Compounds

for Understanding the Impacts of Global Change on Neutral Persistent Organic Pollutants. 33, 469 - 481 (2019).

21. Peng GY, Bellerby R, Zhang F, Sun XR, Li DJ. The ocean's ultimate trashcan: Hadal trenches as major depositories for plastic pollution. Water Research 168, 115121 (2020).

22. Sobek A, et al. Organic matter degradation causes enrichment of organic pollutants in hadal sediments. Nature Communications 14, 2012 (2023).

23. Cui JT, et al. Occurrence of Halogenated Organic Pollutants in Hadal Trenches of the Western Pacific Ocean. Environmental Science & Technology 54, 15821-15828 (2020).

24. Dasgupta S, et al. Toxic anthropogenic pollutants reach the deepest ocean on Earth. Geochemical Perspectives Letters 7, 22-26 (2018).

25. Jamieson AJ, Malkocs T, Piertney SB, Fujii T, Zhang ZL. Bioaccumulation of persistent organic pollutants in the deepest ocean fauna. Nature Ecology & Evolution 1, 0051 (2017).

26. Liu RL, et al. Bulk and Active Sediment Prokaryotic Communities in the Mariana and Mussau Trenches. Frontiers in Microbiology 11, 1521 (2020).

27. Wei H, Liu YH, Huang LT, Wang L, Fang JS, Liu RL. Determining the

abundance, composition and spatial distribution of organohalogens in marine sediments using combustion-ion chromatography. Marine Environmental Research 199,106626 (2024).

28. Xiao WJ, Xu YP, Canfield DE, Wenzhöfer F, Zhang CL, Glud RN. Strong linkage between benthic oxygen uptake and bacterial tetraether lipids in deep-sea trench regions. Nature Communications 15,3439 (2024).

29. Zhang X, et al. The hadal zone is an important and heterogeneous sink of black carbon in the ocean. Communications Earth & Environment 3, 25 (2022).

30. Blum JD, Drazen JC, Johnson MW, Popp BN, Motta LC, Jamieson AJ. Mercury isotopes identify near-surface marine mercury in deep-sea trench biota. Proceedings of the National Academy of Sciences of the United States of America 117, 29292-29298 (2020).

31. Xie JQ, et al. First evidence and potential sources of novel brominated flame retardants and BDE 209 in the deepest ocean. Journal of Hazardous Materials 448,130974 (2023).

32. Luo M, et al. Benthic Carbon Mineralization in Hadal Trenches: Insights From In Situ Determination of Benthic Oxygen Consumption. Geophysical Research Letters 45, 2752-2760 (2018).

33. Xiao WJ, Wang YS, Liu YS, Zhang X, Shi LL, Xu YP. Predominance of

774 hexamethylated 6-methyl branched glycerol dialkyl glycerol tetraethers in the
775 Mariana Trench: source and environmental implication. Biogeosciences 17, 2135-
776 2148 (2020).
777
778 34. Fang H, et al. Metagenomic analysis reveals potential biodegradation pathways of
779 persistent pesticides in freshwater and marine sediments. Science of the Total
780 Environment 470, 983-992 (2014).
781
782 35. Thomas AW, Lewington J, Hope S, Topping AW, Weightman AJ, Slater JH.
783 Environmentally directed mutations in the dehalogenase system of Pseudomonas
784 putida strain PP3. Archives of Microbiology 158, 176-182 (1992).
785
786 36. Zhao Y, Ma J, Zhang L, Tian K, Yao D, Yun Liu. Biodegradation mechanism of
787 organochlorine pesticides: a review. Environ. Prot. Chem. Ind. 41, 551-558 (2021).
788
789 37. Koudelakova T, et al. Substrate specificity of haloalkane dehalogenases. The
790 Biochemical journal 435, 345-354 (2011).
791
792 38. Ngara TR, Zeng PJ, Zhang HJ. mibPOPdb: An online database for microbial
793 biodegradation of persistent organic pollutants. Imeta 1, e45 (2022).
794
795 39. Ruan Z, Xu X, Chen K, Qiao W, Jiang J. Recent advances in microbial
796 catabolism of persistent organic pollutants. 60, 2763-2784 (2020).
797
798 40. Li DD, et al. Quantifying functional redundancy in polysaccharide-degrading

prokaryotic communities. Microbiome 12, 120 (2024).

41. Yang Y, et al. Roles of Organohalide-Respiring Dehalococcoidia in Carbon Cycling. Msystems 5, e00757-e00719 (2020).

42. Adrian L, Löffler F. Organohalide-Respiring Bacteria (2016).

43. Hoshino T, et al. Global diversity of microbial communities in marine sediment. 117, 27587-27597 (2020).

44. Wu JX, et al. Biogeographic distribution, ecotype partitioning and controlling factors of Chloroflexi in the sediments of six hadal trenches of the Paciflc Ocean. Science of the Total Environment 880, 163323 (2023).

45. Futagami T, Morono Y, Terada T, Kaksonen AH, Inagaki F. Dehalogenation Activities and Distribution of Reductive Dehalogenase Homologous Genes in Marine Subsurface Sediments. Applied and Environmental Microbiology 75, 6905-6909 (2009).

46. Futagami T, Morono Y, Terada T, Kaksonen AH, Inagaki F. Distribution of dehalogenation activity in subseafloor sediments of the Nankai Trough subduction zone. Philosophical Transactions of the Royal Society B-Biological Sciences 368, 368 (2013).

47. Xu YP, et al. Distribution, Source, and Burial of Sedimentary Organic Carbon in

Kermadec and Atacama Trenches. Journal of Geophysical Research-Biogeosciences 126, e2020JG006189 (2021).

48. Liu R, et al. Depth-Resolved Distribution of Particle-Attached and Free-Living Bacterial Communities in the Water Column of the New Britain Trench. Front Microbiol 9, 625 (2018).

49. Bolger AM, Lohse M, Usadel B. Trimmomatic: a flexible trimmer for Illumina sequence data. Bioinformatics 30, 2114-2120 (2014).

50. Nurk S, Meleshko D, Korobeynikov A, Pevzner PA. metaSPAdes: a new versatile metagenomic assembler. Genome Research 27, 824-834 (2017).

51. Hyatt D, Chen GL, LoCascio PF, Land ML, Larimer FW, Hauser LJ. Prodigal: prokaryotic gene recognition and translation initiation site identification. Bmc Bioinformatics 11, 119 (2010).

52. Li WZ, Godzik A. Cd-hit: a fast program for clustering and comparing large sets of protein or nucleotide sequences. Bioinformatics 22, 1658-1659 (2006).

53. Kanehisa M, Sato Y, Morishima K. BlastKOALA and GhostKOALA: KEGG Tools for Functional Characterization of Genome and Metagenome Sequences. Journal of Molecular Biology 428, 726-731 (2016).

54. Liu WG, Schmidt B, Müller-Wittig W. CUDA-BLASTP: Accelerating BLASTP

on CUDA-Enabled Graphics Hardware. Ieee-Acm Transactions on Computational Biology and Bioinformatics 8, 1678-1684 (2011).

55. Li H, Durbin R. Fast and accurate short read alignment with Burrows-Wheeler transform. Bioinformatics 25, 1754-1760 (2009).

56. Etherington GJ, Ramirez-Gonzalez RH, MacLean D. bio-samtools 2: a package for analysis and visualization of sequence and alignment data with SAMtools in Ruby. Bioinformatics 31, 2565-2567 (2015).

57. Katoh K, Standley DM. MAFFT Multiple Sequence Alignment Software Version 7: Improvements in Performance and Usability. Molecular Biology and Evolution 30, 772-780 (2013).

58. Capella-Gutiérrez S, Silla-Martínez JM, Gabaldón T. trimAl: a tool for automated alignment trimming in large-scale phylogenetic analyses. Bioinformatics 25, 1972-1973 (2009).

59. Nguyen LT, Schmidt HA, von Haeseler A, Minh BQ. IQ-TREE: A Fast and Effective Stochastic Algorithm for Estimating Maximum-Likelihood Phylogenies. Molecular Biology and Evolution 32, 268-274 (2015).

60. Langmead B, Salzberg SL. Fast gapped-read alignment with Bowtie 2. Nature Methods 9, 357-U354 (2012).

874 61. Kang DD, Froula J, Egan R, Wang Z. MetaBAT, an efficient tool for accurately
875 reconstructing single genomes from complex microbial communities. PeerJ 3, e1165
876 (2015).
877
878 62. Parks DH, Imelfort M, Skennerton CT, Hugenholtz P, Tyson GW. CheckM:
879 assessing the quality of microbial genomes recovered from isolates, single cells, and
880 metagenomes. Genome Research 25, 1043-1055 (2015).
881
882 63. Olm MR, Brown CT, Brooks B, Banfield JF. dRep: a tool for fast and accurate
883 genomic comparisons that enables improved genome recovery from metagenomes
884 through de-replication. Isme Journal 11, 2864-2868 (2017).
885
886 64. Chaumeil PA, Mussig AJ, Hugenholtz P, Parks DH. GTDB-Tk: a toolkit to
887 classify genomes with the Genome Taxonomy Database. Bioinformatics 36, 1925-
888 1927 (2020).
889
890 65. Eddy SR. A new generation of homology search tools based on probabilistic
891 inference. Genome informatics International Conference on Genome Informatics 23,
892 205-211 (2009).
893
894 66. Price MN, Dehal PS, Arkin AP. FastTree 2--approximately maximum-likelihood
895 trees for large alignments. PLoS One 5, e9490 (2010).
896
897 67. Letunic I, Bork P. Interactive tree of life (iTOL) v3: an online tool for the display
898 and annotation of phylogenetic and other trees. Nucleic Acids Research 44, W242-

W245 (2016).

68. Tatusov RL, et al. The COG database: an updated version includes eukaryotes. Bmc Bioinformatics 4, 41 (2003).

69. Seemann T. Prokka: rapid prokaryotic genome annotation. Bioinformatics 30, 2068-2069 (2014).

70. Zhou ZC, et al. METABOLIC: high-throughput profiling of microbial genomes for functional traits, metabolism, biogeochemistry, and community-scale functional networks. Microbiome 10, 33 (2022).

71. Kopylova E, Noé L, Touzet H. SortMeRNA: fast and accurate filtering of ribosomal RNAs in metatranscriptomic data. Bioinformatics 28, 3211-3217 (2012).

914 **Figure legends**

915 **Figure 1.** (A) Locations of sediment cores involved in the analysis of this study. The
916 red stars with squares indicate the stations and samples with detailed geochemical
917 data analyzed. (B) The geochemical parameters of the sediment cores from the
918 Mariana Trench, including the concentrations of adsorbable organic halogens (AOF,
919 AOCl, AOBr and AOX), and the corresponding insoluble organic halogens (IOF,
920 IOCl, IOBr, IOX and IOX), as well as total organic halogen contents (TOBr, TOCl,
921 TOF, and TOX). The values of total organic carbon (TOC) and their carbon isotopic
922 compositions (δ13C), as well the molar ratio of calculated molar ratios of organic
923 carbon to halogen atoms (C:X) were also shown.

924

925 **Figure 2.** (A) Relative abundance of different types of dehalogenases in the
926 metagenomes from the global ocean. The values were expressed as genes per million
927 (GPM). (B) Maximum-likelihood phylogenetic tree of haloalkane dehalogenase
928 identified from the sediment of the Mariana Trench. Red arrows indicate the location
929 of previously characterized haloalkane dehalogenase sequences from the Uniport
930 database. A sequence of epoxide hydrolase (accession no. P07099) was used as the
931 root.

932

933 **Figure 3.** (A) Maximum-likelihood phylogenomic tree of the 143 MAGs containing
934 genes encoding dehalogenase. An archaeal genome (accession no.
935 GCF_004799605.1) was utilized as the root. The colored backgrounds indicate the
936 phylum level classification, and different symbols indicate the types dehalogenase
937 genes each MAGs contained. (B) The relative abundance of each MAG in the
938 metagenomes from different sediment samples of the Mariana Trench. The numbers at

939 the lefthand side indicate the total relative abundance of the 143 MAGs.

940

941 **Figure 4.** The detailed pathways for the HOCs degradation and related

942 biogeochemical cycling by the dehalogenation microbial taxa (the 143 MAGs)

943 identified from the sediment of the Mariana Trench. The name of the encoding gene

944 involved in each step of degradation was shown, and the value in the brackets shows

945 the number of MAGs containing the gene. The pie charts beside the gene names

946 indicate the phylum level classification and proportion of the MAGs containing the

947 gene.

948

949 **Figure 5.** Degradation of typical HOCs compounds by microbial community from the

950 sediment of the Mariana Trench, tested using the simulated high-pressure microcosms

951 (A) Decreasing of both substrates with incubation time in the treatments with intact

952 trench sediments. (B) Relative abundance (GPM) and transcription activities (TPM)

953 of the MAGs containing dehalogenase during different times of the incubation. (C)

954 and (D), relative abundance and transcription activities of functional genes related

955 with pathways for degradation of HOCs.

956

957

Fig. 1

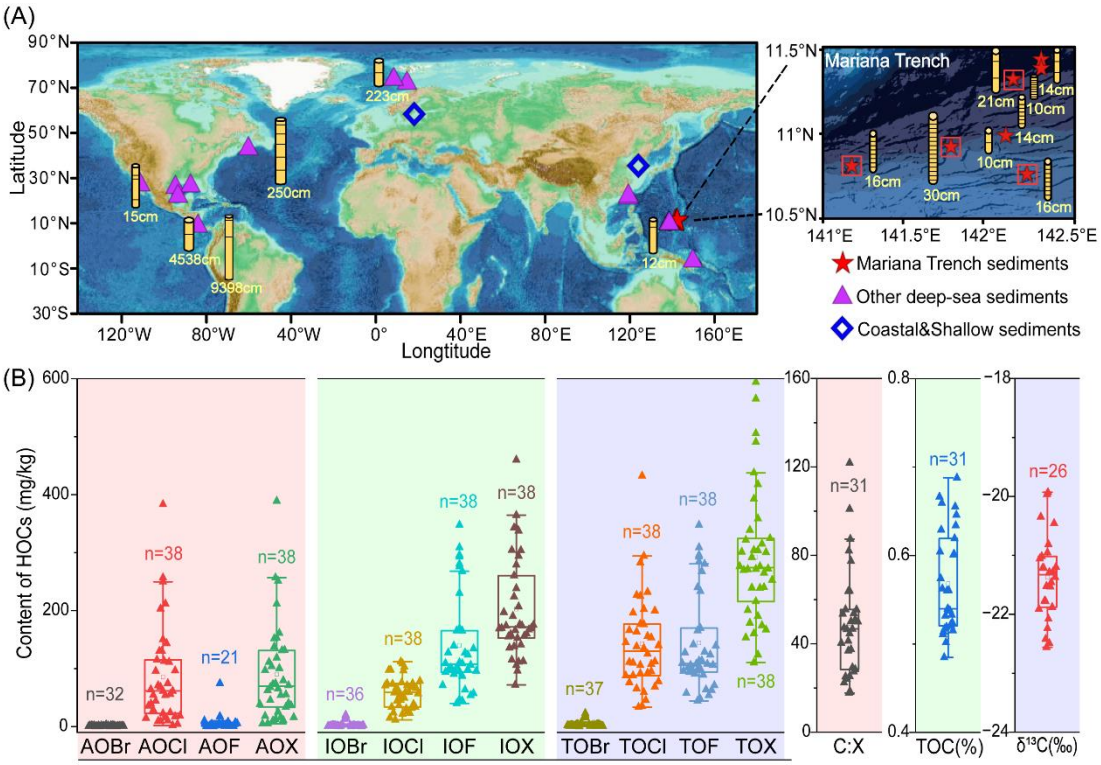
(A)
Latitude
Longtitude
90°N
70°N
50°N
30°N
10°N
10°S
30°S
120°W
80°W
40°W
0°
40°E
80°E
120°E
160°E
223cm
250cm
15cm
4538cm
9398cm
125cm
Mariana Trench
11.5°N
11°N
10.5°N
141°E
141.5°E
142°E
142.5°E
21cm
14cm
10cm
14cm
10cm
16cm
30cm
16cm
Mariana Trench sediments
Other deep-sea sediments
Coastal&Shallow sediments
(B)
Content of HOCs (mg/kg)
n=32
n=38
n=21
n=38
n=36
n=38
n=38
n=37
n=38
n=38
n=38
n=31
n=31
n=26
AOBr
AOCl
AOF
AOX
IOBr
IOCl
IOF
IOX
TOBr
TOCl
TOF
TOX
C:X
TOC(%)
δ13C(‰)

962 **Fig. 2**

963

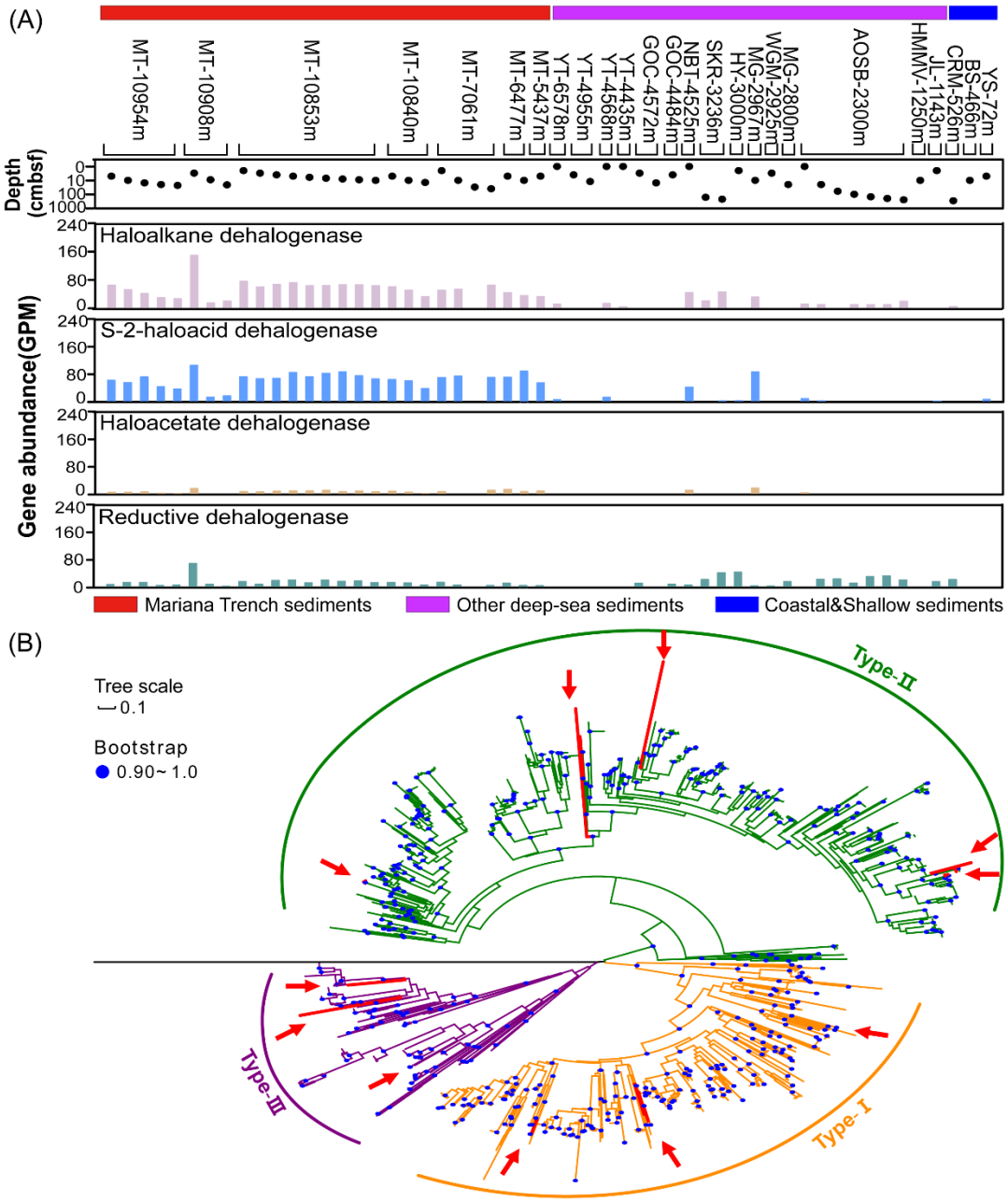

964

965

966

967

968

969

Fig. 3

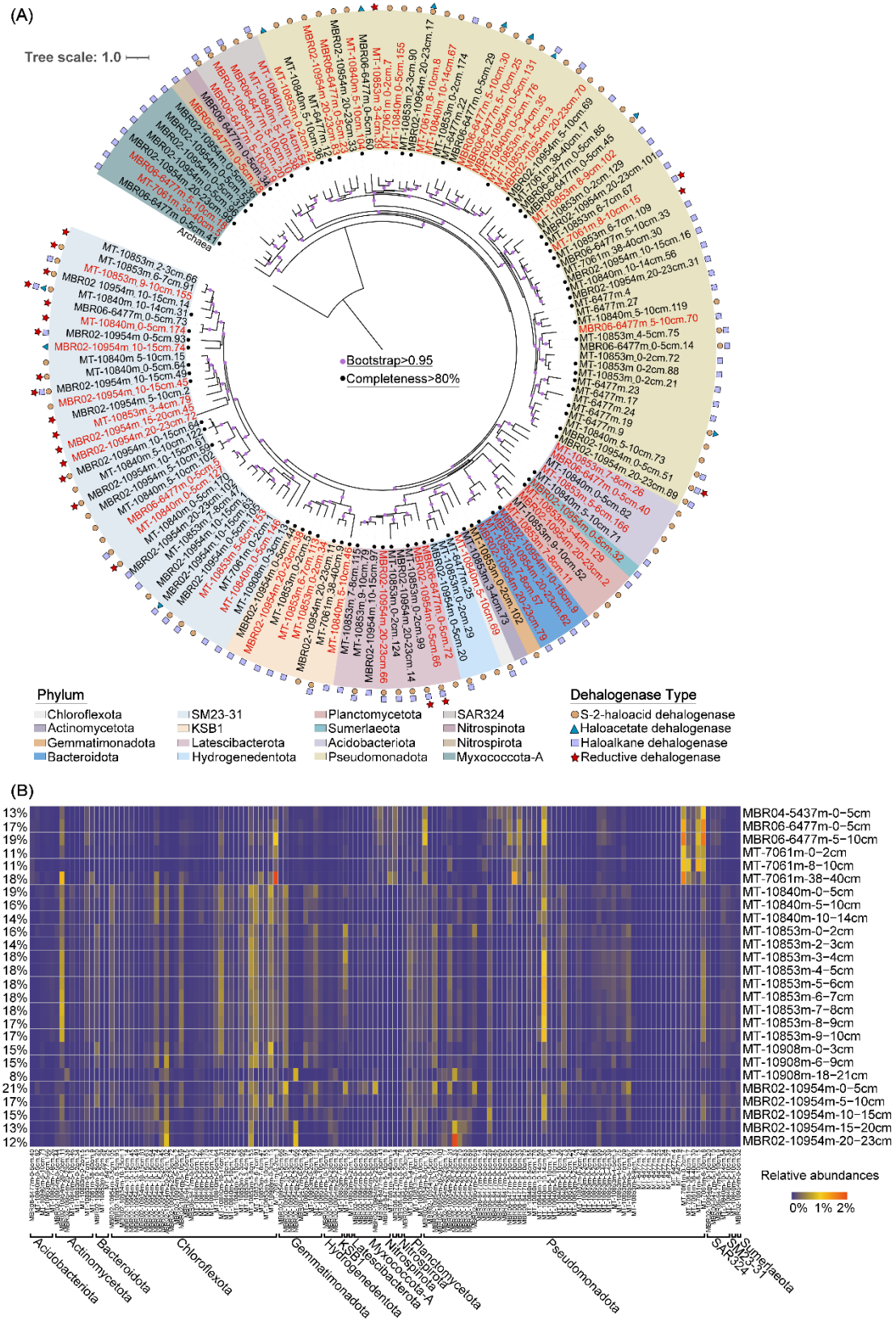
(A)
Tree scale: 1.0
Archaea
Bootstrap>0.95
Completeness>80%
Phylum
Chloroflexota
Actinomycetota
Gemmatimonadota
Bacteroidota
SM23-31
KSB1
Latescibacterota
Hydrogenedentota
Planctomycetota
Sumerlaeota
Acidobacteriota
Pseudomonadota
SAR324
Nitrospinota
Nitrospirota
Myxococcota-A
Dehalogenase Type
S-2-haloacid dehalogenase
Haloacetate dehalogenase
Haloalkane dehalogenase
Reductive dehalogenase
(B)
MBR04-5437m-0-5cm
MBR06-6477m-0-5cm
MBR06-6477m-5-10cm
MT-7061m-0-2cm
MT-7061m-8-10cm
MT-7061m-38-40cm
MT-10840m-0-5cm
MT-10840m-5-10cm
MT-10840m-10-14cm
MT-10853m-0-2cm
MT-10853m-2-3cm
MT-10853m-3-4cm
MT-10853m-4-5cm
MT-10853m-5-6cm
MT-10853m-6-7cm
MT-10853m-7-8cm
MT-10853m-8-9cm
MT-10853m-9-10cm
MT-10908m-0-3cm
MT-10908m-6-9cm
MT-10908m-18-21cm
MBR02-10954m-0-5cm
MBR02-10954m-5-10cm
MBR02-10954m-10-15cm
MBR02-10954m-15-20cm
MBR02-10954m-20-23cm
Relative abundances
0% 1% 2%
Acidobacteriota
Actinomycetota
Bacteroidota
Chloroflexota
Gemmatimonadota
Hydrogenedentota
KSB1
Latescibacterota
Myxococcota-A
Nitrospinota
Nitrospirota
Planctomycetota
Pseudomonadota
SAR324
SM23-31
Sumerlaeota

Fig. 4

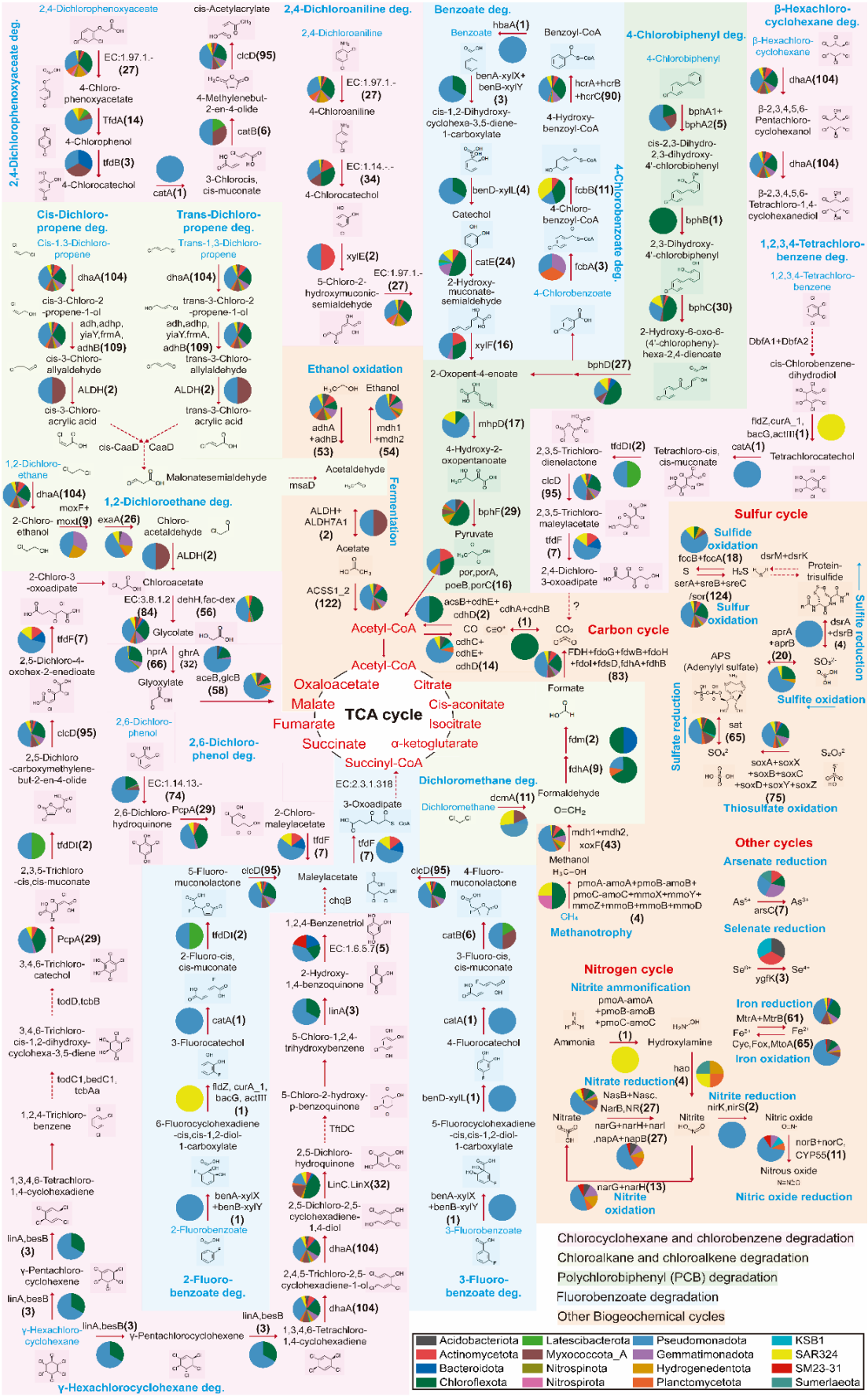
2,4-Dichlorophenoxyaceate deg.
2,4-Dichlorophenoxyaceate
4-Chloro-phenoxyacetate
4-Chlorophenol
4-Chlorocatechol
EC:1.97.1.-(27)
TfdA(14)
tfdB(3)
cis-Acetylacrylate
4-Methylenebut-2-en-4-olide
3-Chlorocis, cis-muconate
clcD(95)
catB(6)
catA(1)
2,4-Dichloroaniline deg.
2,4-Dichloroaniline
4-Chloroaniline
4-Chlorocatechol
5-Chloro-2-hydroxymuconic-semialdehyde
EC:1.97.1.-(27)
EC:1.14.-.-(34)
xylE(2)
Benzoate deg.
Benzoate
Benzoyl-CoA
hbaA(1)
benA-xylX+benB-xylY(3)
cis-1,2-Dihydroxy-cyclohexa-3,5-diene-1-carboxylate
4-Hydroxy-benzoyl-CoA
hcrA+hcrB+hcrC(90)
benD-xylL(4)
Catechol
fcbB(11)
4-Chloro-benzoyl-CoA
catE(24)
2-Hydroxy-muconate-semialdehyde
fcbA(3)
4-Chlorobenzoate
xylF(16)
4-Chlorobiphenyl deg.
4-Chlorobiphenyl
bphA1+bphA2(5)
cis-2,3-Dihydro-2,3-dihydroxy-4'-chlorobiphenyl
bphB(1)
2,3-Dihydroxy-4'-chlorobiphenyl
bphC(30)
2-Hydroxy-6-oxo-6-(4'-chlorophenyl)-hexa-2,4-dienoate
bphD(27)
4-Chlorobenzoate deg.
β-Hexachloro-cyclohexane deg.
β-Hexachloro-cyclohexane
dhaA(104)
β-2,3,4,5,6-Pentachloro-cyclohexanol
β-2,3,4,5,6-Tetrachloro-1,4-cyclohexanediol
1,2,3,4-Tetrachloro-benzene deg.
1,2,3,4-Tetrachloro-benzene
DbfA1+DbfA2
cis-Chlorobenzene-dihydrodiol
fldZ,curA_1,bacG,actIII(1)
catA(1)
Tetrachlorocatechol
Cis-Dichloro-propene deg.
Cis-1,3-Dichloro-propene
cis-3-Chloro-2-propene-1-ol
adh,adhp,yiaY,frmA,adhB(109)
cis-3-Chloro-allyaldehyde
ALDH(2)
cis-3-Chloro-acrylic acid
Trans-Dichloro-propene deg.
Trans-1,3-Dichloro-propene
trans-3-Chloro-2-propene-1-ol
trans-3-Chloro-allylaldehyde
trans-3-Chloro-acrylic acid
cis-CaaD
CaaD
Ethanol oxidation
Ethanol
adhA+adhB(53)
mdh1+mdh2(54)
Acetaldehyde
msaD
Malonatesemialdehyde
1,2-Dichloro-ethane
dhaA(104)
moxF+moxI(9)
2-Chloro-ethanol
1,2-Dichloroethane deg.
exaA(26)
Chloro-acetaldehyde
ALDH(2)
Fermentation
ALDH+ALDH7A1(2)
Acetate
ACSS1_2(122)
2-Chloro-3-oxoadipate
Chloroacetate
EC:3.8.1.2(84)
dehH,fac-dex(56)
Glycolate
tfdF(7)
2,5-Dichloro-4-oxohex-2-enedioate
hprA(66)
ghrA(32)
Glyoxylate
aceB,glcB(58)
clcD(95)
2,5-Dichloro-carboxymethylene-but-2-en-4-olide
2,6-Dichloro-phenol
2,6-Dichloro-phenol deg.
EC:1.14.13.-(74)
2,6-Dichloro-hydroquinone
PcpA(29)
2-Chloro-maleylacetate
tfdF(7)
tfdDI(2)
2,3,5-Trichloro-cis,cis-muconate
PcpA(29)
3,4,6-Trichloro-catechol
todD,tcbB
3,4,6-Trichloro-cis-1,2-dihydroxy-cyclohexa-3,5-diene
todC1,bedC1,tcbAa
1,2,4-Trichloro-benzene
1,3,4,6-Tetrachloro-1,4-cyclohexadiene
linA,besB(3)
γ-Pentachloro-cyclohexene
linA,besB(3)
γ-Hexachloro-cyclohexane
γ-Hexachlorocyclohexane deg.
linA,besB(3)
γ-Pentachlorocyclohexene
linA,besB(3)
1,3,4,6-Tetrachloro-1,4-cyclohexadiene
Acetyl-CoA
Acetyl-CoA
Oxaloacetate
Citrate
Malate
Fumarate
TCA cycle
Cis-aconitate
Isocitrate
Succinate
α-ketoglutarate
Succinyl-CoA
EC:2.3.1.318
3-Oxoadipate
tfdF(7)
5-Fluoro-muconolactone
clcD(95)
Maleylacetate
chqB
clcD(95)
4-Fluoro-muconolactone
1,2,4-Benzenetriol
EC:1.6.5.7(5)
2-Hydroxy-1,4-benzoquinone
linA(3)
5-Chloro-1,2,4-trihydroxybenzene
5-Chloro-2-hydroxy-p-benzoquinone
TftDC
2,5-Dichloro-hydroquinone
LinC,LinX(32)
2,5-Dichloro-2,5-cyclohexadiene-1,4-diol
dhaA(104)
2,4,5-Trichloro-2,5-cyclohexadiene-1-ol
dhaA(104)
2-Fluoro-cis, cis-muconate
tfdDI(2)
catA(1)
3-Fluorocatechol
fldZ, curA_1, bacG, actIII(1)
6-Fluorocyclohexadiene-cis,cis-1,2-diol-1-carboxylate
benA-xylX+benB-xylY(1)
2-Fluorobenzoate
2-Fluoro-benzoate deg.
catB(6)
3-Fluoro-cis, cis-muconate
catA(1)
4-Fluorocatechol
benD-xylL(1)
5-Fluorocyclohexadiene-cis,cis-1,2-diol-1-carboxylate
benA-xylX+benB-xylY(1)
3-Fluorobenzoate
3-Fluoro-benzoate deg.
Dichloromethane deg.
Dichloromethane
dcmA(11)
Formaldehyde
O=CH2
Formate
fdm(2)
fdhA(9)
Carbon cycle
CO
CO2
cdhA+cdhB(1)
cdhC+cdhE+cdhD(14)
FDH+fdoG+fdwB+fdoH+fdoI+fdsD,fdhA+fdhB(83)
?
2,3,5-Trichloro-dienelactone
clcD(95)
tfdDI(2)
Tetrachloro-cis, cis-muconate
2,3,5-Trichloro-maleylacetate
tfdF(7)
2,4-Dichloro-3-oxoadipate
bphF(29)
Pyruvate
por,porA,poeB,porC(16)
acsB+cdhE+cdhD(2)
mhpD(17)
4-Hydroxy-2-oxopentanoate
2-Oxopent-4-enoate
Sulfur cycle
Sulfide oxidation
fccB+fccA(18)
S
H2S
serA+sreB+sreC/sor(124)
Sulfur oxidation
dsrM+dsrK
Protein-trisulfide
Sulfite reduction
aprA+aprB(20)
dsrA+dsrB(4)
APS (Adenylyl sulfate)
Sulfite oxidation
Sulfate reduction
sat(65)
SO4
soxA+soxX+soxB+soxC+soxD+soxY+soxZ(75)
Thiosulfate oxidation
Other cycles
Arsenate reduction
As5+
arsC(7)
As3+
Selenate reduction
Se6+
ygfK(3)
Se4+
Iron reduction
MtrA+MtrB(61)
Fe3+
Fe2+
Cyc,Fox,MtoA(65)
Iron oxidation
Methanol
mdh1+mdh2,xoxF(43)
pmoA-amoA+pmoB-amoB+pmoC-amoC+mmoX+mmoY+mmoZ+mmoB+mmoD(4)
CH4
Methanotrophy
Nitrogen cycle
Nitrite ammonification
pmoA-amoA+pmoB-amoB+pmoC-amoC
Ammonia
(1)
Hydroxylamine
hao
Nitrate reduction(4)
NasB+Nasc.NarB,NR(27)
narG+narH+narI,napA+napB(27)
Nitrate
Nitrite
Nitrite reduction
nirK,nirS(2)
Nitric oxide
norB+norC,CYP55(11)
Nitrous oxide
narG+narH(13)
Nitrite oxidation
Nitric oxide reduction
Chlorocyclohexane and chlorobenzene degradation
Chloroalkane and chloroalkene degradation
Polychlorobiphenyl (PCB) degradation
Fluorobenzoate degradation
Other Biogeochemical cycles
Acidobacteriota
Actinomycetota
Bacteroidota
Chloroflexota
Latescibacterota
Myxococcota_A
Nitrospinota
Nitrospirota
Pseudomonadota
Gemmatimonadota
Hydrogenedentota
Planctomycetota
KSB1
SAR324
SM23-31
Sumerlaeota

Fig. 5

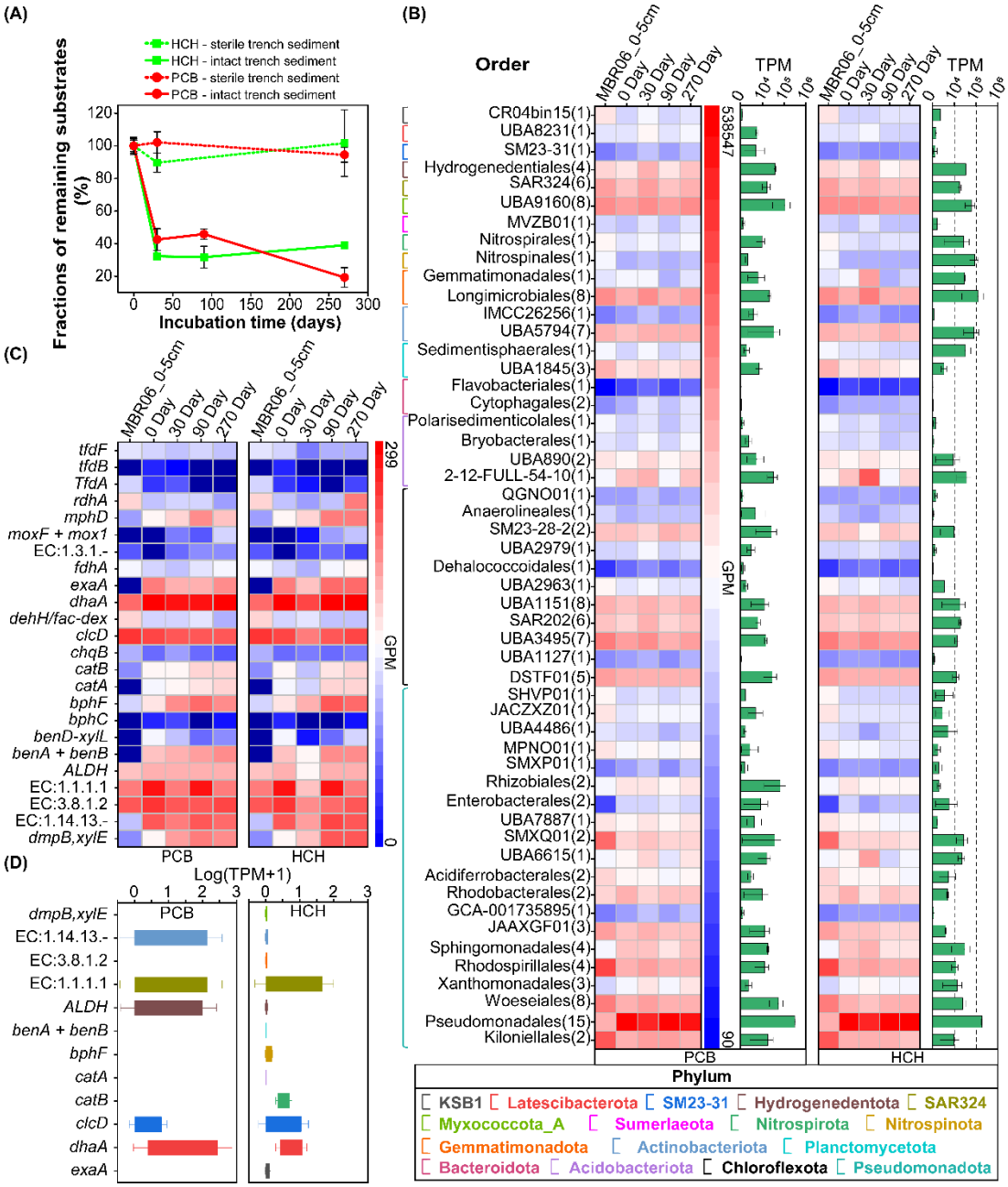
(A)
HCH - sterile trench sediment
HCH - intact trench sediment
PCB - sterile trench sediment
PCB - intact trench sediment
Fractions of remaining substrates (%)
Incubation time (days)
(B)
Order
MBR06_0-5cm
0 Day
30 Day
90 Day
270 Day
TPM
GPM
PCB
HCH
Phylum
KSB1
Latescibacterota
SM23-31
Hydrogenedentota
SAR324
Myxococcota_A
Sumerlaeota
Nitrospirota
Nitrospinota
Gemmatimonadota
Actinobacteriota
Planctomycetota
Bacteroidota
Acidobacteriota
Chloroflexota
Pseudomonadota
(C)
tfdF
tfdB
TfdA
rdhA
mphD
moxF + mox1
EC:1.3.1.-
fdhA
exaA
dhaA
dehH/fac-dex
clcD
chqB
catB
catA
bphF
bphC
benD-xylL
benA + benB
ALDH
EC:1.1.1.1
EC:3.8.1.2
EC:1.14.13.-
dmpB,xylE
(D)
Log(TPM+1)